LAWRENCE
LIVERMORE
NATIONAL
LABORATORY

LLNL-CONF-517471

# Event-by-event evaluation of the prompt fission neutron spectrum from 239Pu(n,f)

R. Vogt, J. Randrup, D. A. Brown, M. A. Descalle, W. E. Ormand

November 30, 2011

NEDPC
Los Alamos, NM, United States
October 17, 2011 through October 21, 2011

## Disclaimer

# Event-by-event evaluation of the prompt fission neutron spectrum from $^{239}$Pu(n,f) (U)

*R. Vogt[1], J. Randrup[2], D. A. Brown[1], M.-A. Descalle[1] and W. E. Ormand[1]*

[1]*LLNL, Livermore, CA, USA*

[2]*LBNL, Berkeley, CA, USA*

***We have developed an improved evaluation method for the spectrum of neutrons emitted in fission of $^{239}$Pu induced by incident neutrons with energies up to 20 MeV. The <ν> covariance data, including incident energy correlations introduced by the <ν> evaluation method, were used to fix the input parameters in our event-by-event model of fission, FREYA, by applying formal statistical methods. Formal estimates of uncertainties in the evaluation were developed by randomly sampling model inputs and calculating likelihood functions based on agreement with the evaluated <ν>. Our approach is able to employ a greater variety of fission measurements than the relatively coarse spectral data alone. It also allows the study of numerous fission observables for more accurate model validation. The combination of an event-by-event Monte Carlo fission model with a statistical-likelihood analysis is thus a powerful tool for evaluation of fission-neutron data.***

***Our empirical model FREYA follows the complete fission event from birth of the excited fragments through their decay via neutron emission until the fragment excitation energy is below the neutron separation energy when neutron emission can no longer occur. The most recent version of FREYA incorporates pre-equilibrium neutron emission, the emission of the first neutron before equilibrium is reached in the compound nucleus, and multi-chance fission, neutron evaporation prior to fission when the incident neutron energy is above the neutron separation energy. Energy, momentum, charge and mass number are conserved throughout the fission process. The best available values of fragment masses and total kinetic energies are used as inputs to FREYA. We fit three parameters that are not well under control from previous measurements: the shift in the total fragment kinetic energy; the energy scale of the asymptotic level density parameter, controlling the fragment `temperature' for neutron evaporation; and the relative excitation of the light and heavy fragments, governing the number and energy of neutrons emitted from each fragment. The latter two parameters are assumed to be independent of the incident neutron energy while the first varies with incident energy.***

***We describe our method and the subsequent spectral evaluation and present the results of several standard validation calculations that test our new evaluation. These benchmarks include critical assemblies, sensitive to criticality in fast systems; pulsed sphere measurements testing the spectra at incident neutron energies of 14 MeV; and other tests. (Unclassified)***

## Introduction

One of the most important quantities involved in fission applications is the prompt fission neutron spectrum (PFNS). The experimental spectral data themselves are neither sufficiently accurate nor of sufficiently consistent quality to produce an improved PFNS evaluation. However, by combining measured information about the nuclear fragment yields and energies with the very precise evaluations of neutron multiplicities, it is possible to constrain the neutron spectrum rather tightly without having to rely on the spectral data.

Our approach employs the fission model FREYA (Fission Reaction Event Yield Algorithm) that incorporates the relevant physics through the use of previously measured observables and relevant modeling[1,2,3,4]. FREYA simulates the entire fission process, producing a large sample of complete fission

events with full kinematic information on the emerging fission products and the emitted neutrons and photons. It is also fast, producing 1M events in 12 s on a laptop. It incorporates the pre-fission emission of neutrons from the fissile compound nucleus as well as sequential neutron evaporation from the fission fragments. FREYA is thus a potentially powerful tool for bridging the gap between current microscopic models and important fission observables and for improving estimates of the relatively gross fission characteristics important for applications.

Heretofore, most fission simulations have assumed that all emitted neutrons are drawn from the same energy spectrum, precluding correlations between the neutron multiplicity and the associated spectral shape. In our event-by-event treatment, such inherent correlations are automatically included. Thus FREYA goes well beyond the average fission model. In the remainder of this paper, we describe how FREYA works, how it differs from the average fission model, and how it is being used to produce evaluations.

## Model Description

FREYA follows each fission event from the birth of the excited fragments through their decay via prompt neutron emission until the fragment excitation energy is below the neutron separation energy. It also includes the subsequent gamma emission from each fragment, albeit in a rather preliminary way.

We assume binary fission of the compound nucleus, *e.g.* $^{240}$Pu, with mass $A_c$ and charge $Z_c$ formed by incident neutrons of energy $E_n$ on an actinide with mass $A_c$ - *1*, *e.g.* $^{239}$Pu. The identities of the hot, excited fission fragments are obtained by sampling the mass and charge of the light, $L$, or heavy, $H$, fragment from fission fragment distributions. To ensure mass and charge conservation, if i.e. the heavy fragment is chosen, $A_L = A_c - A_H$ and $Z_L = Z_c - Z_H$. Once the fragments have been sampled, the fission $Q$ value is determined from their mass and charge and is subsequently divided into the total fragment kinetic and excitation energies. We take the shape of the total fragment kinetic energy as a function of heavy fragment mass, TKE($A_H$), from available data for thermal neutron-induced fission. We assume the shape of TKE($A_H$) is independent of energy, see Fig. 1. The total fragment excitation energy, TEE, for a given $Q$ value is found using energy conservation, TEE = $Q$ – TKE. The TEE is then divided between the light and heavy fragments and translated into a fragment temperature assuming $E^* = a\, T_{LH}^2$ where $a = A_i/e_0$ and $e_0$ is the asymptotic level density parameter. To go beyond the equal temperature situation, we adjust the relative excitation energies of the light and heavy fragments, maintaining the same overall value of TEE. Allowing for temperature fluctuations in small systems, we modify the excitation energies by their thermal fluctuations. Since accounting for fluctuations may change the TEE, we introduce corresponding fluctuations in TKE to retain total energy conservation. Neutrons are evaporated from the excited fragments until the excitation energy is too low for further neutron emission. Prompt gamma emission follows after prompt neutron emission ceases.

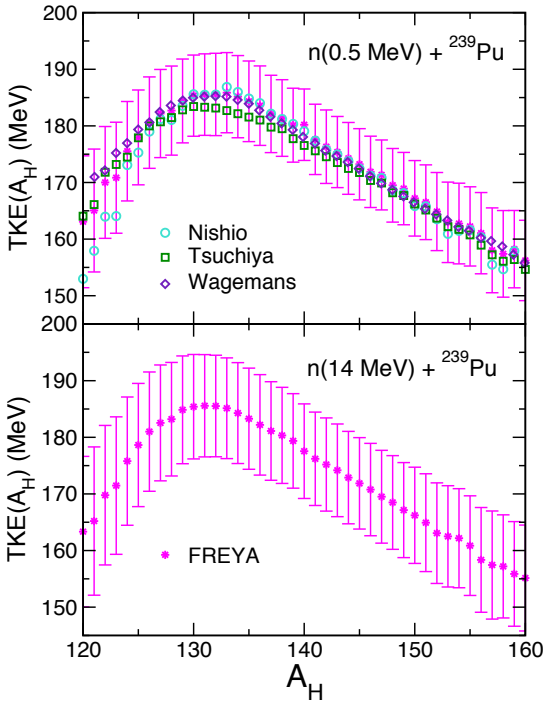


Figure 1 **TKE($A_H$) for thermal neutron induced fission[5,6,7] compared to FREYA results[4] at 0.5 and 14 MeV. The vertical bars are the variances of the calculated results, not statistical uncertainties.**

For FREYA to produce a spectral evaluation for incident neutron energies, $E_n$, up to 20 MeV, additional physics processes must be included for incident neutron energies of greater than a few MeV. We now briefly describe this physics.

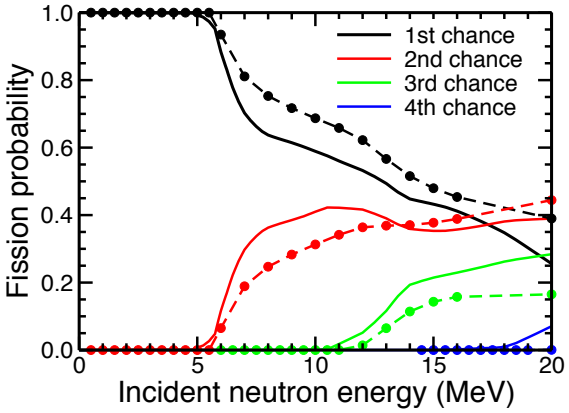


Figure 2 **The probability for first (black), second (red), third (green) and fourth (blue) chance fission as a function of the incident neutron energy. The solid curves are GNASH results while the dashed curves with dots are the FREYA results[3].**

As the energy of the incident neutron increases, neutron evaporation from the compound nucleus becomes competitive with direct or first-chance fission. The competition between fission and neutron evaporation can be quantified as the ratio between the decay widths for neutron evaporation and fission as a function of the excitation energy of the compound nucleus, $\Gamma_n(E^*)/\Gamma_f(E^*)$. Neutron evaporation is possible whenever the excitation energy of the compound nucleus exceeds the neutron separation energy, $E^* > S_n$. (Since it costs energy to remove a neutron from the nucleus, $S_n$ is positive.) The excitation of the evaporation daughter nucleus is $E_f^* = E^* - S_n - Q_{\rm rel}$ where $Q_{\rm rel}$ is the kinetic energy of the relative motion between the emitted neutron and the daughter nucleus. If $Q_{\rm rel}$ exceeds the fission barrier in the daughter nucleus, then second-chance fission is possible, as is the emission of an additional neutron prior to possible fission of the resulting daughter nucleus. Thus as the incident neutron energy is raised, the emission of an ever-increasing number of pre-fission neutrons becomes possible and the associated fission events may be classified as first-chance fission (when there are no pre-fission neutrons emitted), second-chance fission (when one neutron is emitted prior to fission), and so on. The resulting fission probabilities as a function of incident neutron energy are given in Fig. 2.

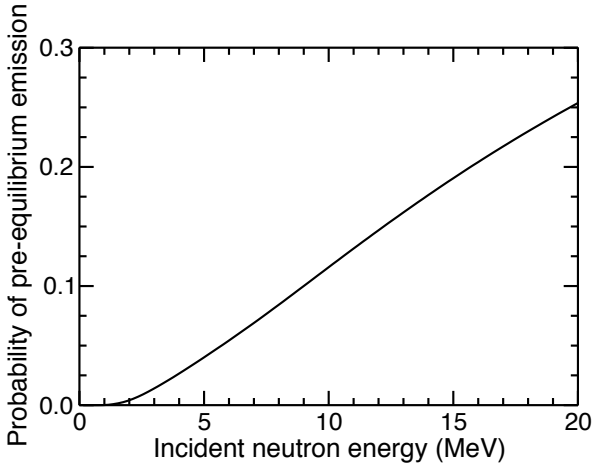


Figure 3 **The probability for pre-equilibrium neutron emission as a function of the incident neutron energy[3].**

When the incident neutron energy is increased above a few MeV, there is a growing chance that equilibrium is not established before the first pre-fission neutron is emitted. Under such circumstances the calculation of statistical neutron evaporation must be augmented by a suitable non-equilibrium treatment. We employ a two-component exciton model that describes the evolution of the nuclear reaction in terms of time-dependent populations of ever more complex many-particle-many-hole states. The calculated probability for pre-equilibrium neutron emission is shown in Fig. 3 as a function of $E_n$. While practically negligible below a few MeV, the probability for pre-equilibrium emission grows approximately linearly with $E_n$ to about 24% at 20 MeV. In each generated event, FREYA first considers the possibility of pre-equilibrium neutron emission and, if it occurs, a neutron is emitted with an energy selected from the calculated pre-equilibrium spectrum. Subsequently, the possibility of equilibrium neutron evaporation is considered, starting either from the original agitated compound nucleus, $^{240}$Pu, or the less excited nucleus, $^{239}$Pu, remaining after pre-equilibrium emission has

occurred. Neutron evaporation is iterated until the excitation energy of the final daughter nucleus is below the fission barrier (in which case the event is abandoned and a new event is generated) or the compound nucleus fissions before (further) neutron evaporation can occur.

Finally, the fragment mass yields, $Y(A)$, are energy dependent. The yields are assumed to exhibit three distinct Gaussian modes,

$$Y(A) = S_1(A) + S_2(A) + S_L(A) .$$

The first two terms represent asymmetric fission modes associated with the spherical shell closure at $N = 82$ and the deformed shell closure at $N = 88$, respectively, while the last term represents a broad symmetric mode. The symmetric mode is relatively insignificant for low $E_n$ but grows in importance with energy. In addition, above the threshold for multi-chance fission, these lower excitation energy contributions must also be taken into account. As a result, at higher $E_n$, the tails of $Y(A)$ broaden and the dip at symmetric fission, $A_c/2$, begins to fill in, see Fig. 4.

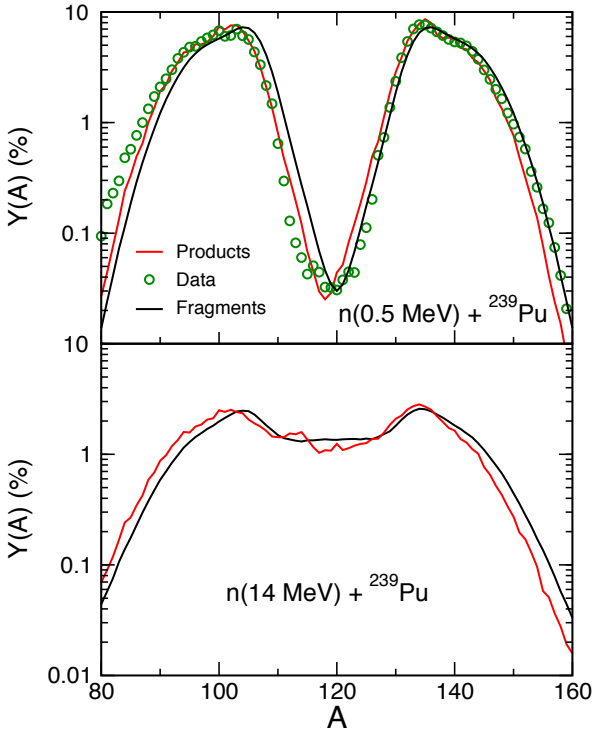


Figure 4 **The fragment (black) and product (red) yields as a function of fragment mass[4].**

## FREYA Parameters

To obtain the best possible agreement between the neutron multiplicity and the neutron spectra, three FREYA parameters have been tuned to the very accurate measurements of $<\nu>$. The first, $d$TKE, depends on the incident neutron energy, the other two, $e_0$ and $x$, are assumed to be independent of energy. In more detail, they describe the:

- shift of TKE($A_H$), $d$TKE, from the average of the measured TKE values at thermal energies, $E_{th}$. The shape is assumed to be independent of energy since shell effects do not set in until incident energies well above 20 MeV so that TKE($A_H$,$E_n$) = TKE($A_H$,$E_{th}$) + $d$TKE. Note that $d$TKE can be either positive or negative.
- asymptotic level density parameter, $e_0$. The level density parameter, $a$, sets the fragment temperature for neutron evaporation. The asymptotic form, $a = A/e_0$, was used by Madland and Nix[8]. FREYA employs the back-shifted Fermi gas expression for the level density, dependent on both the mass and charge of the fragment $i$ as well as the excitation energy,
  $a_i(E_i^*) = (A_i/e_0)[1 + (\delta W_i/U_i)(1 - e^{-\gamma U_i})]$ ,
  where $U_i = E_i^* - \Delta_i$, $\Delta_i$ is the fragment pairing energy, $\delta W_i$ is the shell correction, and $\gamma = 0.05$. If shell corrections are negligible, $\delta W \sim 0$ and $a_i \sim A_i/e_0$.
- relative excitation of the light and heavy fragments, $x$. Observations suggest that light fragments are more excited, leading to higher multiplicities than that due to statistical partition of the excitation energies ($x = 1$). We take $E'^*_L = x\,E^*_L$; $E'^*_H$ = TEE – $E'^*_L$. Note that if $x > 1$, more neutrons are evaporated from the light fragment than the heavy fragment.

The dependence of $\nu$ on fragment mass number is very sensitive to the value of $x$. All measurements of $\nu(A)$ exhibit a characteristic 'sawtooth' behavior: the neutron multiplicity from the light fragment increases slowly as $A$ approaches $A_c/2$ and then drops to a minimum near $A \sim 130$, the same location as the

maximum of TKE($A_H$). Due to the closed shell near that $A$, the fragments are particularly resistant to neutron emission. Past the dip, the multiplicity increases again. The FREYA results provide a rather good representation of the available data, even though the model is not tuned to them, see Fig. 5.

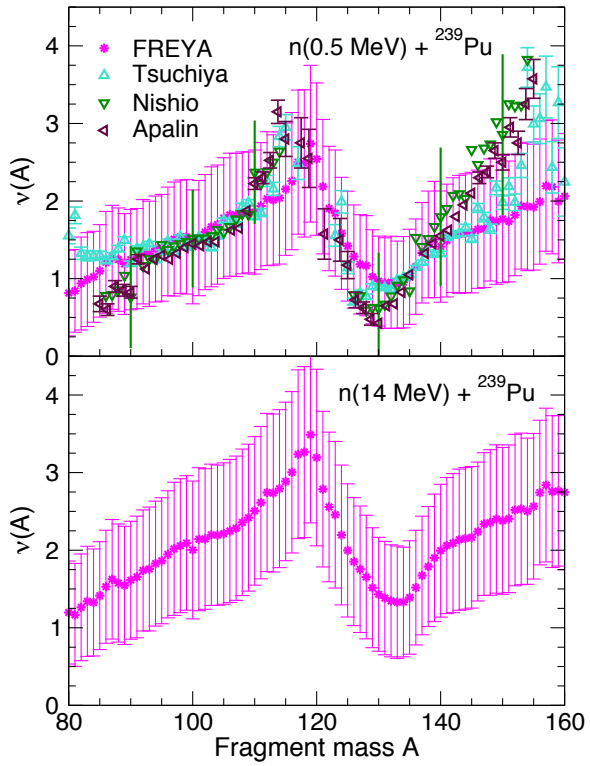


Figure 5 **The neutron multiplicity as a function of $A$ for $E_n$ = 0.5 MeV[5,6,9] and 14 MeV. The vertical green bars at $\Delta A$ =10 in the top plot are the full width half maximum of the distribution in neutron multiplicity of the Z range available for that $A$. The FREYA results[4] also include this variance.**

## Differences between FREYA and an 'average' fission model

Since FREYA simulates complete fission events through prompt emission, it conserves energy and momentum of the fragments as well as the neutrons and gammas emitted from the de-excitation of the fragments. We assume that the fully accelerated fission fragments first de-excite by neutron emission, presumably sequential emission from each fragment, followed by sequential gamma emission. At each stage of this process, the spectral shape of the ejectile is determined by the maximum temperature of the daughter nucleus, determined in turn by the excitation of the emitting nucleus and the associated $Q$ values for the particular fragment species. Because there are many possible $Q$ values for each fission event and because the excitation of the mother fragment nucleus fluctuates, the temperature distribution in the daughter is nontrivial. The temperature distribution from a single fragment is shown in Fig. 6 for $E_n$ = 0.5 and 14 MeV. The higher excitation energy at 14 MeV manifests itself in the broader peak in $P(T)$ at higher $T$ for $\nu$ = 1 and larger overall probabilities for higher residual temperatures with 2 and 3 emitted neutrons. The shape of $P(T)$ is not triangular, as assumed in Ref. 8.

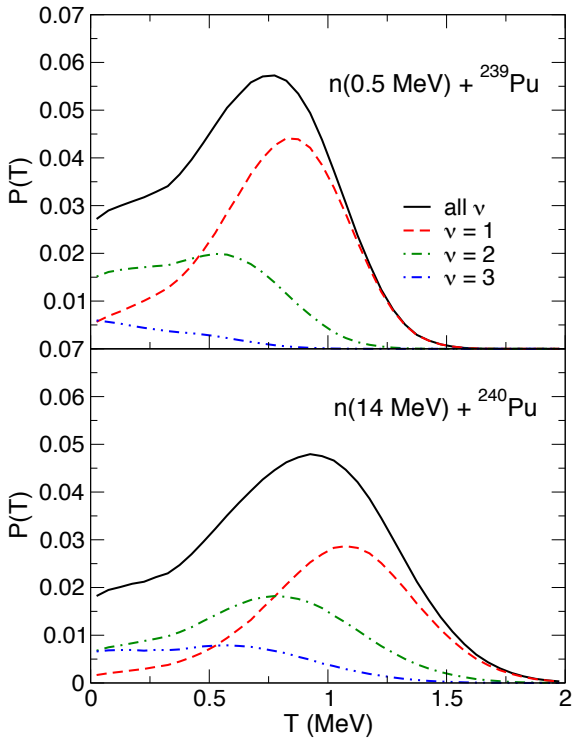


Figure 6 **The distribution of the maximum temperature in the residual nucleus, $P(T)$, after $\nu$ neutrons have been evaporated. The curves show the results for $\nu$ = 1 (dashed), 2 (dot-dashed) and 3 (dot-dot-dashed) as well as the sum of all neutron emission (solid)[4].**

The decrease in the residual temperature of the daughter nuclei, shown in Fig. 6, manifests itself in other, more convenient, observables. The spectral shapes, $f_\nu(E) = (1/\nu)(d\nu/dE)$, normalized to unity, reflect these temperature changes directly. There is a definite softening of the spectra seen with increasing neutron multiplicity, as may be expected when the available excitation energy is shared between more neutrons, especially for the lower incident neutron energy. This feature, a consequence of energy-momentum conservation, is not accounted for when neutrons are sampled from the same, multiplicity-independent spectral shape. In addition, there is a 'kink' in the 14 MeV spectral shape occurring at the difference in energy between the incident neutron energy and the neutron separation energy, $E_n - S_n$, ~ 8.4 MeV for $E_n$ = 14 MeV. While the 'kink' in $f_\nu$ is small averaged over all multiplicities, the change in the spectral shape gated on neutron multiplicity is significant, see Fig. 7.

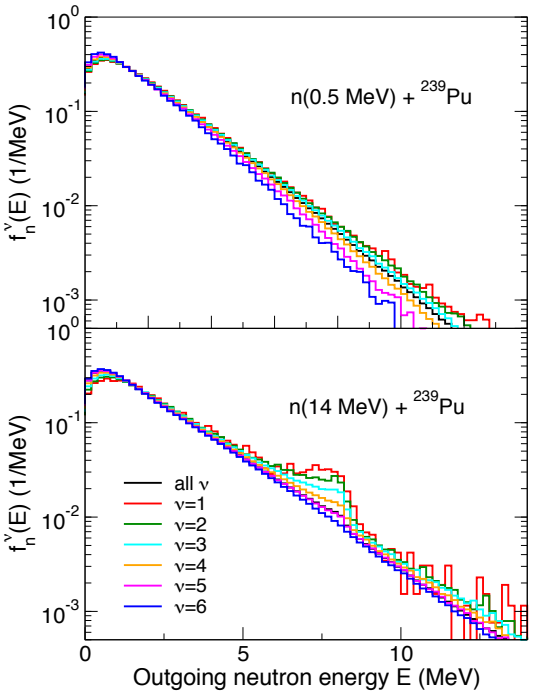


Figure 7 **The spectral shape of prompt fission neutrons from neutron-induced fission for events with fixed neutron multiplicity[4]. (The higher multiplicity results in a more steeply falling spectrum.)**

Finally, we show the neutron multiplicity distribution, $P(\nu)$. Each neutron emission reduces the excitation energy in the residual nucleus not only by the kinetic energy of the neutron, $\langle E \rangle = 2T$, but also by the (significantly larger) neutron separation energy $S_n$. The resulting $P(\nu)$ is considerably narrower than a Poisson distribution with the same average multiplicity, as shown in Fig. 8.

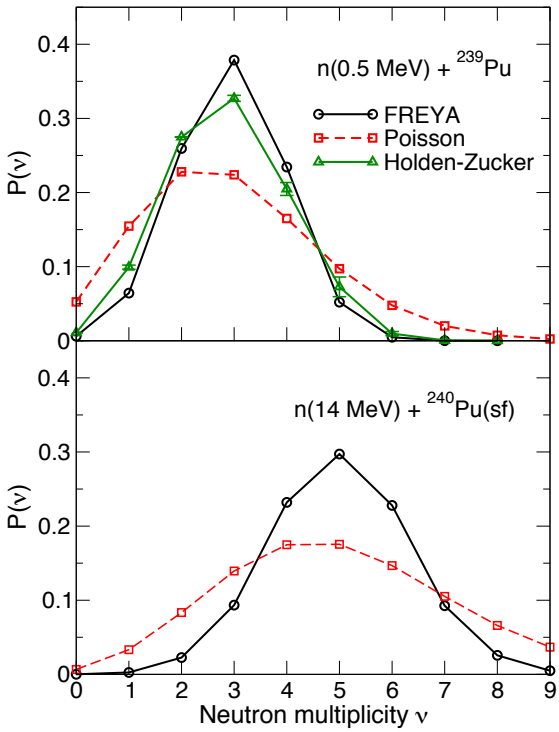


Figure 8 **The neutron multiplicity distributions for neutron-induced fission at 0.5 MeV and 14 MeV. The FREYA results[4] are given by the black solid curves while the equivalent Poisson distribution is shown in the red dashed curves. The composite Holden-Zucker result[10] compares well to that of FREYA.**

## Making an evaluation

We use a Monte Carlo approach to Bayesian inference (inverse problem theory) to obtain the fit parameters $\{d\mathrm{TKE}(E_n), e_0, x\}$ and, thus, the spectral evaluation. As previously stated, we assume that $e_0$ and $x$ are independent of incident neutron energy. We vary $d$TKE linearly between fixed points chosen

to map contours of $<\nu>(E_n)$ and reasonably cover the multi-chance fission thresholds. We fit to $<\nu>$ for twenty different energies between $10^{-11}$ and 20 MeV. At each energy value, a set of *d*TKE values, together with the values of $e_0$ and $x$ for this realization, are generated. The parameter values are evenly distributed in parameter space. We generate 1M FREYA events for all 20 values of incident neutron energy and compare the value of $<\nu>$ obtained at each $E_n$ to that of the $<\nu>$ evaluation in ENDF/B-VII[11], taking the energy-energy covariance of the evaluated $<\nu>$ into account. The best estimate of the parameter values is obtained from the likelihood-weighted average of all parameter sets at all energies; the best fit is that with the largest likelihood. We produce an evaluation based on this best fit; test against critical assemblies, pulsed sphere measurements and other available data; and repeat if necessary.

## Summary

Event-by-event fission studies with FREYA are a significant step forward in modeling since they encompass the full range of mass and charge partitions while conserving energy and momentum at each stage of the fission process. It is thus possible to study a wide range of observables, including correlations.

There is, however, still much room for improvement, particularly where input data are concerned. Most experiments focus on one aspect of the fission process – fragments, prompt neutrons or prompt gammas – instead of all three due to detector limitations. Most neutron measurements, such as $\nu(A)$ and $P(\nu)$, are only available at thermal energies. Higher energy measurements would validate (or not) some of our assumptions concerning the energy dependence of *e.g.* TKE($A_H$). In addition, the spectral data themselves are often inconsistent with each other and have large uncertainties, especially at low and high outgoing neutron energies. While improved models can make up for some deficiencies, the upcoming measurements with modern detectors such as the fission TPC and ChiNu will be very important.

## Acknowledgments

This work was performed under the auspices of the U.S. Department of Energy by Lawrence Livermore National Laboratory under Contract DE-AC52-07NA27344 (RV, DAB, MAD, WEO), by Lawrence Berkeley National Laboratory under Contract DE-AC02-05CH11231 (JR) and was also supported in part by the National Science Foundation Grant NSF PHY-0555660 (RV).

## References

1. Randrup J and Vogt R, "Calculation of fission observables through event-by-event simulation", Phys. Rev. C **80,** 024601 (2009).

2. Vogt R, Randrup J, Pruet J, and Younes W, "Event-by-event study of prompt neutrons from $^{239}$Pu$(n,f)$", Phys. Rev. C **80**, 044611 (2009).

3. Vogt R, Randrup J, Brown D A, Descalle M A, and Ormand W E, "Event-by-event evaluation of the prompt fission neutron spectrum from $^{239}$Pu$(n,f)$", arXiv:1105.4655.

4. Vogt R and Randrup J, "Event-by-event study of neutron observables in spontaneous and thermal fission", Phys. Rev. C **84**, 044621 (2011).

5. Nishio K, Nakagome Y, Kanno I, and Kimura I, "Measurement of fragment mass dependent kinetic energy and neutron multiplicity for thermal neutron induced fission of $^{239}$Pu", J. Nucl. Sci. Technol. **32**, 404 (1995), http://www-nds.iaea.org/exfor/servlet/X4sGetSubent?subID=23012006; http://www-nds.iaea.org/exfor/servlet/X4sGetSubent?subID=23012005.

6. Tsuchiya C, Nakagome Y, Yamana H, Moriyama H, Nishio K, Kanno I, Shin K, and Kimura I, "Simultaneous measurement of prompt neutrons and fission fragments for $^{239}$Pu$(n_{th},f)$", J. Nucl. Sci. Technol. **37**, 941 (2000), http://www-nds.iaea.org/exfor/servlet/X4sGetSubent?subID=22650003; http://www-nds.iaea.org/exfor/servlet/X4sGetSubent?subID=2260005.

7. Wagemans C, Allaert E, Deruytter A, Barthelemy R, and Schillebeeckx P, "Comparison of the energy and mass characteristics of the $^{239}$Pu$(n_{th},f)$ and the $^{240}$Pu(sf) fragments", Phys. Rev. C **30**, 218 (1984), http://www-nds.iaea.org/exfor/servlet/X4sGetSubent?subID=21995038.

8. Madland D G and Nix J R, "New calculation of prompt fission neutron spectra and average prompt neutron multiplicities", Nucl. Sci. Eng. **81**, 213 (1982).

9. Apalin V F, Gritsyuk Yu N, Kutikov I E, Lebedev V I, and Mikaelian L A, "Neutron emission from $^{233}$U, $^{235}$U and $^{239}$Pu fission fragments", Nucl. Phys. A **71**, 553 (1965), http://www-nds.iaea.org/exfor/servlet/X4sGetSubent?subID=41397002.

10. Holden N E and Zucker M S, "A reevaluation of the average prompt neutron emission multiplicity (nubar) values from fission of uranium and transuranium nuclides", BNL-NCS-35513, 1985.

11. Chadwick M B, *et al.*, "ENDF/B-VII.0: Next generation evaluated nuclear data library for nuclear science and technology", Nucl. Data Sheets **107**, 2931 (2006).